Flame Fronts in Iron Suspensions Dominated by the Effect of Discreteness

Sam Goroshin, Francois-David Tang, Andrew J. Higgins
Department of Mechanical Engineering, McGill University
Montreal, Quebec, Canada

1 Introduction

Propagating diffusion fronts in reactive, heterogeneous media consisting of two spatially separated phases are common in many fields such as chemical kinetics, combustion, biology, etc. [1]. The reaction in such systems is localized within or at the phase boundaries and thus the source term in the governing reaction-diffusion equation is not a continuous spatial function, i.e., it is discrete. Often, the approach used for obtaining traveling wave solutions in such discrete systems is to average (homogenize) the source term with a spatially continuous function [2]. However, a homogeneous representation of the sources is justified only if the two characteristic scales of the propagating diffusion wave, the width of the reaction zone $l_R = vt_R$ and the width of the diffusion zone $l_D = D/v$, are much larger than the scale of the system heterogeneity l (here v is the front velocity, t_R is the characteristic time of reaction, and D is the active component diffusivity) [3, 4]. Because length scales are functions of the propagation speed, they cannot be estimated *a priori* from a solution that uses a yet unjustified source homogenization procedure [5].

To investigate the validity of the homogenization approach to model the diffusion front in a system with discrete sources, we will obtain in the present work an exact solution for the front speed without spatial averaging of sources and will compare it to a known solution derived from a mean-field theory approach. We will show that in a system with regularly distributed sources, discreteness leads to the appearance of a specific front propagation limit with non-zero front speed even if the diffusing component produced by the sources is conserved (i.e., no losses are present). Finally, we will show experimentally that the continuous and discrete propagation regimes using the same reactive system can be achieved by changing the diffusivity of the active component.

In our analysis, we will consider the simplest possible discrete system where the sources of the diffusing component are points embedded in an inert continuum. We will also assume the source term to be a stepwise function in time: the source turns on when the diffusing component reaches some prescribed value T_i and then releases the active component with constant rate for a prescribed period of time t_R. In spite of its simplicity, such a discrete source model has a physical analog: a flame in suspensions of a non-volatile solid fuel in a gaseous oxidizer [3], in which case the active component released by the sources is heat. Indeed, due to the density difference between the solid fuel and gas of more than three orders of magnitude, the distance between fuel particles in a combustible suspension is much larger than

Correspondence to: samuel.goroshin@mcgill.ca

their diameter such that the particles can be approximated as point sources. The ignition temperature T_i of particles is, in the first approximation, independent of flame speed [2]. Furthermore, the particle reaction time t_R after ignition is controlled by the O_2 diffusion towards the particle surface [6], and as a first approximation, the diffusivity is independent of the temperature. Using terminology common to combustion, the three dimensionless parameters characterizing the problem can be identified as the ignition temperature $\theta_i = c_p \rho T_i/(QB)$ (Q is the heat release per unit mass of fuel, B is the fuel mass per unit volume of mixture, c_p is the specific heat of the mixture, and ρ is the density of the media), the flame speed $\eta = vl/D$ (v is flame speed, l is the distance between particles and D is the thermal diffusivity of the media), and the combustion time $\tau_c = t_R D/l^2$.

2 Modeling

2.1 Analytical Model for Regular Systems

To begin, we will show a solution of the above formulated problem that approximates the heat sources by a spatially continuous function. The expression defining flame speed in homogeneous media with a stepwise reaction rate is well known [3] and can be written using dimensionless parameters defined above as follows:

$$\theta_i = \frac{1 - e^{-\eta^2 \tau_c}}{\eta^2 \tau_c}. \tag{1}$$

Equation (1) contains only one combination of dimensionless parameters $\eta^2 \tau_c$ that does not depend on l, the distance between particles, because the heat source term has been spatially homogenized. The dependence of η on τ_c is plotted in Fig. 1 as solid lines. The flame speed decreases as θ_i increases and tends to zero in the limit of $\theta_i = 1$. In other words, if the heat released by the reaction is able to increase the temperature of the media to its ignition point T_i, a reactive wave will propagate. In the limit where the reaction temperature just reaches ignition, the flame speed approaches zero. Hereafter, this condition (i.e., adiabatic flame temperature $T_A = QB/(c_p \rho)$ equals ignition temperature T_i) will be referred to as the thermodynamic limit.

To obtain an analytical expression for the flame speed in the same system without invoking source averaging, we initially assume that the distribution of particles forms a three-dimensional, regular lattice. We also assume that the flame propagates in the x-direction from left to right and all particles in the $z - y$ plane ignite simultaneously, i.e., the flame front is flat. Due to linearity of the heat diffusion equation, the temperature of a plane of particles just about to be ignited ($x = 0$) can be found by linear superimposition of the contributions from all reacted and still reacting particles on the left side of the domain:

$$T_i = T_o + \sum_{i=1}^{\infty} \sum_{j=-\infty}^{\infty} \sum_{k=-\infty}^{\infty} \Delta T_{ijk} \tag{2}$$

When the reaction time is small in comparison to the characteristic time of the heat transfer between particles, i.e., $\tau_c = t_R D/l^2 << 1$, all particles on the left side of the igniting plane are already reacted at the moment of ignition. In this case, reacted particles (sources) can be approximated by δ-functions not only in space but also in time ($\tau_c \to 0$) and ΔT_{ijk} is simply the Green's function for an individual particle:

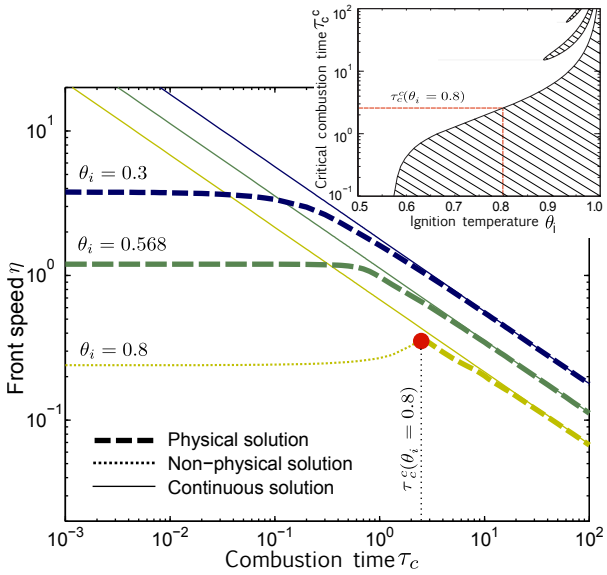

Figure 1: Dependence of the flame speed η on the combustion time τ_c in a system with regularly-spaced point-like heat sources for $\theta_i = 0.3, 0.568$ and 0.8. The solid line represents the homogeneous approach from Eq. (1), the long dash line represents the physical solution to Eq. (5) and the short dotted line is the unphysical solution to Eq. (5). The inset shows the dependence of the critical combustion time τ_c^c on the ignition temperature θ_i. The hatched region indicates where flame propagation is no longer possible.

$$\Delta T_{ijk} = \frac{Q}{c_p \rho} \frac{1}{(4\pi D i \Delta\tau)^{3/2}} \exp\left(\frac{\left(i^2+j^2+k^2\right) l^2}{4Di\Delta\tau}\right) \tag{3}$$

Here we assume that consecutive planes of particles are ignited at regular time intervals $\Delta\tau$ so the time elapsed from the ignition of the i-th row can be written as $i\Delta\tau$. By combining Eqs. (2) and (3), the flame speed in the suspension of instantly reacting particles can be written using dimensionless parameters as:

$$\theta_i = \frac{1}{(4\pi)^{3/2}} \sum_{i=1}^{\infty} \sum_{j=-\infty}^{\infty} \sum_{k=-\infty}^{\infty} \left(\frac{\eta}{i}\right)^{3/2} \exp\left(\frac{\left(i^2+j^2+k^2\right)\eta}{4i}\right) \tag{4}$$

For an arbitrary combustion time $\tau_c \geq 0$, Eq. (4) can be written in the general form using the integral over time of the Green's functions:

$$\theta_i = \frac{1}{(4\pi\tau_c)^{3/2}} \sum_{i=1}^{\infty} \sum_{j=-\infty}^{\infty} \sum_{k=-\infty}^{\infty} \int_{\left(\frac{i}{\eta}-\tau_c\right)\Theta\left(\frac{i}{\eta}-\tau_c\right)}^{\frac{i}{\eta}} \tau^{-3/2} \exp\left(-\frac{i^2+j^2+k^2}{4\tau}\right) d\tau \tag{5}$$

where Θ is the Heaviside function accounting for particles that are still burning at the moment of ignition. Unlike in the homogeneous approximation given by Eq. (1), the flame speed defined by Eqs. (4)

and (5) explicitly depends on the structure of the media, i.e., on the inter-particle spacing l. For the limiting case of instantly reacting particles ($\tau_c = 0$) given by Eq. (4), it is inversely proportional to l but the dependence diminishes with increasing dimensionless reaction time τ_c. Therefore τ_c is the measure of the system's departure from the homogeneous case: the system demonstrates discrete properties when $\tau_c << 1$ and becomes homogeneous when $\tau_c >> 1$. The identification of the discreteness parameter τ_c now provides a quantitative tool that determines when spatial averaging is a valid procedure. Just as spatial averaging may not be justified in certain systems, the existence of heterogeneity in the media through which the reactive wave propagates is not sufficient grounds to reject the use of spatial averaging. Only by examining the discreteness parameter τ_c can the appropriateness of spatial averaging be evaluated.

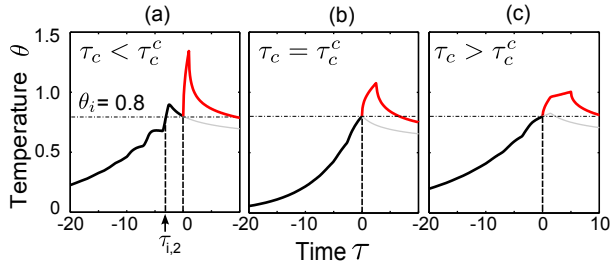

Figure 2: Time-temperature histories of a particle igniting under (a) physically invalid ($\tau_c = 0.1$), (b) critical ($\tau_c = 2.57$), and (c) physically valid ($\tau_c = 5$) conditions. The ignition temperature is $\theta_i = 0.8$ in all cases. The thin gray line originating at $\tau = 0$ corresponds to the particle temperature if ignition is omitted.

The flame speed η expressed by Eq. (5) is in good agreement with Eq. (1) when $\tau_c >> 1$, but, while Eq. (1) predicts that η tends to infinity as τ_c approaches zero, the solution obtained by Eq. (5) is insensitive to τ_c and asymptotes towards a finite value given by Eq. (4). When θ_i exceeds ~ 0.568, the solution to Eqs. (4) and (5) becomes unphysical when the combustion time τ_c is below some critical value τ_c^c. Detailed analytical examination of the temperature history of the particles reveals that the particle ignites at $\tau = 0$ as the temperature decreases, ignoring the earlier ignition event at $\tau_{i,2}$ in the increasing branch of the same temperature curve, as shown in Fig. 2(a). If the particles are allowed to react upon first reaching their ignition temperature, the sequencing of regular ignition events required by this analytic solution is disrupted. If the requirement of a constant delay time between the ignition of particle planes is relaxed, numerical simulations of the resulting propagation dynamics shows that the front promptly quenches. As further evidence of unphysical characteristics, the flame speed η increases with τ_c when $\tau_c < \tau_c^c$ as shown in Fig. (1). The onset of unphysical propagation at τ_c^c is indicative of propagation limit and is encountered at a finite speed, in contrast to the thermodynamic limit associated with Eq. (1), which states that the flame speed η goes to 0 when θ_i tends to 1, irrespectively of τ_c. The critical combustion time τ_c^c, separating physical (Fig. 2(c)) and unphysical ignition conditions (Fig. 2(a)) is a function of θ_i. For $\theta_i \approx 0.568$, the critical combustion time is $\theta_c^c = 0$ and the corresponding flame speed is $\eta = 1.2$. The critical combustion time τ_c^c tends to infinity and the critical flame speed η_c approaches zero asymptotically as θ_i tends to unity as shown in the inset of Fig. 1. Near the propagation limit, the flame is unstable and transient numerical simulation of the flame fronts near the critical limit reveals behavior that is typical for bifurcating solutions prior to extinction: period doubling of ignition delay times followed by onset of the chaotic behavior [4, 7]. The system also demonstrates increasingly complex behavior near the propagation limit when $\theta_i > 0.9$ where physical and unphysical propagation regions often alternate (see inset in Fig. 1) [7]. Equations (4) and (5) can be applied to a 1-D system of equally spaced planar sources and 2-D arrays of line sources if we note that the summations in the j and

k components can be approximated by integrations over planar and line sources, respectively. Thus, the propagation limit found here applies equally regardless of the dimensions of the system.

We emphasize that the failure of the wave at τ_c^c occurs in the absence of heat losses to the system. Even when the quantity released by the sources is conserved (i.e., heat in the case of combustion), the propagation limit is encountered at values of ignition temperature below the thermodynamic limit and at non-zero flame speed, which is in contrast to models that homogenize the sources and predict the thermodynamic limit discussed above. We attribute this phenomenon to the discrete nature of the sources resulting in heat diffusing outward from each source in all directions (including opposite to the direction of propagation), whereas in a homogenized model, heat only diffuses toward unreacted media. Propagation beyond this limit (which was found here for regular arrays) is only possible via random distribution in the positions of the sources. This possibility (i.e., the wave exploiting local concentration fluctuations to continue propagation) means that propagation limits in random media can only be defined probabilistically.

2.2 Numerical Simulations with Random Systems

To explore the effect of randomizing the spatial positioning of the sources (in contrast to the analytic solution with the regular lattice presented previously), simulations in systems with randomly distributed point sources were investigated by the method of superimposing the Green's function of individual sources. Computer simulations were performed in 2-D square and 3-D cubic domains containing 8100 and 15 625 point sources, respectively. While numerical simulations were required to examine a statistically significant number of randomly generated systems with a large number of particles, the method of solution remained based on the analytic solution for point sources (i.e., superposition of Green's functions) and no finite difference or other numerical approximations were introduced. Periodic boundary conditions were simulated on the side boundaries of the domain by strategically placing images of reacting sources outside the domain while the front and back boundaries remained free. The initiation of the propagating front was performed by a forced ignition of a layer of sources of variable width. Snapshots of the resulting propagating fronts are shown in Figs. 3(a) and 3(b) for the discrete and continuous regimes, respectively. Significant roughening of the front can be observed for the discrete regime of propagation.

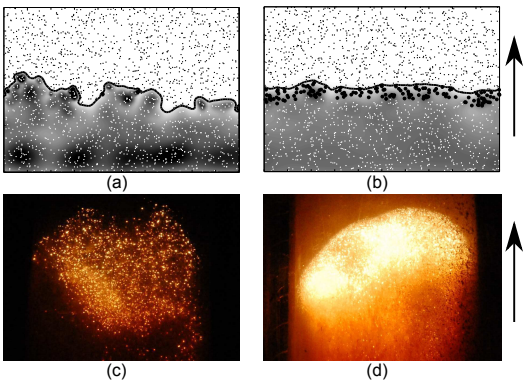

Figure 3: Two-dimensional numerical simulations and photographs of the flame front in iron suspension in Xe-O_2 [(a) and (c)] and He-O_2 [(b) and (d)] mixtures. The upward arrows indicate the propagation direction. The simulations were performed for $\theta_i = 0.206$ and using $\tau_c = 0.4$ and 3.2 in (a) and (b), respectively.

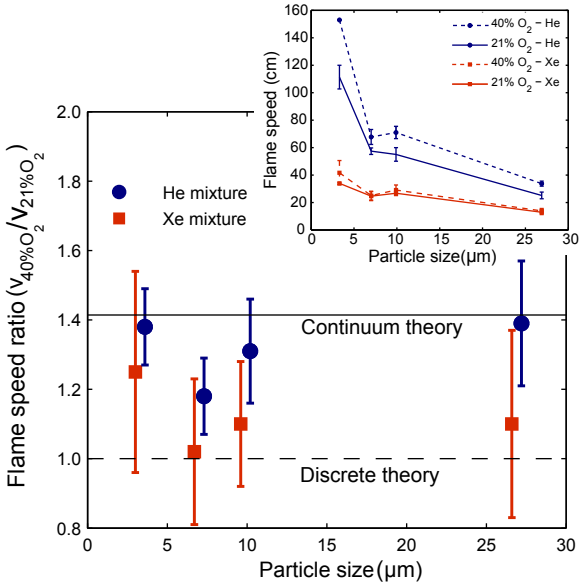

Figure 4: Ratio of flame speeds between two different O_2 concentrations in He and Xe mixtures. The insert shows experimental measurements of the flame speed in iron suspensions in 21% and 40% O_2 in He and Xe.

3 Experiment and Discussion

Both continuous and discrete propagation regimes were realized experimentally in suspensions of iron dust particles in a gaseous oxidizer. At moderate O_2 concentrations, iron particles in suspensions react completely heterogeneously without any gaseous products [8] matching the model assumption of point-like heat sources. By replacing N_2 in air first by He and then by Xe, the thermal diffusivity can be drastically altered, changing the value of the dimensionless combustion parameter τ_c by almost an order of magnitude from 3.2 (predominantly continuous flame propagation regime, $\tau_c > 1$) to 0.4 (predominantly discrete propagation regime, $\tau_c < 1$) without changing the reaction chemistry or adiabatic flame temperature. These values of τ_c were used in the simulations shown in Figs. 3(a) and 3(b).The experiments were performed in reduced gravity created inside an aircraft flying a parabolic trajectory at gravity levels below 0.05 g. Reduced gravity eliminated particle settling and natural convection, allowing observation of low speed flames ($v \approx 5$ cm/s) characteristic for 25 μm iron particles in Xe-O_2 mixtures. The local, particle-to-particle nature of the discrete regime for iron suspensions in Xe-O_2 was manifested by the "rough" front structure, whereas the flame front in He-O_2 mixtures was smooth, characteristic of continuous flames (see Fig. 3). A similar difference in front appearance for He and Xe mixtures was demonstrated by the numerical model as shown in Fig. 3.

Beside the flame appearance, the insensitivity of the flame speed to particle combustion time corroborates the discrete propagation regime in Xe-O_2 mixtures as shown in Fig. 4. Flames in Xe mixtures are less sensitive to changes on the O_2 concentration C_{O_2}, or the particle combustion time ($t_R \sim \frac{1}{C_{O2}}$), suggesting that the propagation mechanism is limited by particle-to-particle heat diffusion, characteristic of discrete flames, whereas flames in He mixtures varied with the O_2 concentration in better agreement with the continuum theory ($v \sim \frac{1}{\sqrt{t_R}}$).

This work is supported by the Canadian Space Agency and was enabled by computing resources provided by WestGrid and Compute/Calcul Canada.

References

[1] J. Xin. *SIAM Review*, 42:161, 2000.

[2] S. Goroshin, M. Bidabadi, and J. H. S. Lee. *Combust. Flame*, 105:147, 1996.

[3] S. Goroshin, J. H. S. Lee, and Y. Shoshin. *Symp. (Int.) Combust.*, 27:743, 1998.

[4] J. M. Beck and V. Volpert. *Physica D*, 182:86, 2003.

[5] N. Provatas, T. Ala-Nissila, M. Grant, K. R. Elder, and L. Piche. *Phys. Rev. E*, 51:4232, 1995.

[6] D.A. Frank-Kamenetskii. *Diffusion and Heat Transfer in Chemical Kinetics*. Princeton University Press, 1955.

[7] F. D. Tang, A. J. Higgins, and S. Goroshin. *Combust. Theor. Model.*, 13:319, 2009.

[8] F. D. Tang, S. Goroshin, A. J. Higgins, and J. H. S. Lee. *Proc. Combust. Inst.*, 32:1905, 2009.